

Optimal 4-Ary Imbalanced-Phase-Amplitude Modulation in Uncorrelated and Correlated Receive Diversity PLC Systems Under Nakagami- m Noise Environment

Soumya P. Dash , *Member, IEEE*, Ranjan K. Mallik , *Fellow, IEEE*, and Badri Ramanjaneya Reddy 

Abstract—A receive diversity power line communication (PLC) system subject to correlated multipath channel fading and corrupted by additive Nakagami- m background noise is considered. The optimal receiver employing a 4-ary imbalanced-phase-amplitude modulation (I-PAM) scheme for data transmission is obtained, using which closed form expressions for the symbol error probability (SEP) in the union bound sense and the SEP in the asymptotic sense at high signal-to-noise ratio (SNR) are derived. The diversity order of the system is found to be independent of the shape parameter of the additive noise. Furthermore, the optimal 4-ary I-PAM constellation minimizing the SEP at lower SNR values is computed numerically. The optimal 4-ary I-PAM constellation is found to be elliptical in shape as opposed to the traditional circular QPSK constellation generally employed in wireless communication systems. The effects of the correlation among the multipath channel gains and the shape parameter of the noise on the optimality of the considered constellation are also presented via numerical studies.

Index Terms—4-ary imbalanced-phase-amplitude modulation, coherent detection, optimal constellation, power line communication (PLC), quadrature phase-shift keying (QPSK), receive diversity, symbol error probability (SEP).

I. INTRODUCTION

POWER line communication (PLC), relying on the transfer of communication data over a pre-existing network of power cables, has attracted the attention of researchers over the past few decades owing to the extensive utilization of the technology towards applications such as control and automation of smart and micro-grid systems, development of communication protocols for smart metering systems, and various other

Manuscript received December 18, 2020; revised April 17, 2021; accepted May 20, 2021. Date of publication May 25, 2021; date of current version July 20, 2021. The work of Soumya P. Dash was supported by the Science and Engineering Research Board (SERB), Government of India, through its Start-up Research Grant (SRG) under Grant SRG/2019/001234. The work of Ranjan K. Mallik was supported in part by the Science and Engineering Research Board, a Statutory Body of the Department of Science and Technology, Government of India, under the J. C. Bose Fellowship. The review of this article was coordinated by Prof. Rui Dinis. (*Corresponding author: Soumya P. Dash.*)

Soumya P. Dash and Badri Ramanjaneya Reddy are with the School of Electrical Sciences, Indian Institute of Technology - Bhubaneswar, Khordha, Odisha 752050, India (e-mail: soumyapdash@iitbbs@gmail.com; badriraman123@gmail.com).

Ranjan K. Mallik is with the Department of Electrical Engineering, Indian Institute of Technology - Delhi, New Delhi 110016, India (e-mail: rk-mallik@ee.iitd.ernet.in).

Digital Object Identifier 10.1109/TVT.2021.3083066

automotive and multimedia applications [1]–[5]. Although PLC technology has such pervasive application areas, reliable data transmission via power line cables still remains as one of the challenging aspects in these scenarios owing to the unconventional nature of the power line channels and noise corrupting the channel. This provides the motivation to researchers to come up with novel transceiver design schemes to mitigate the effect of the unreliable channel characteristics in PLC systems [6], [7].

The PLC channel, as studied in numerous literature, is mostly affected by multiplicative and additive noises. Similar to the wireless communications scenario, multiplicative noise in PLC channels arises due to the multipath effect on the transmitting data due to the presence of multiple reflections of the data symbols from the nodes in the power line network leading to impedance mismatch in the circuit [1]. There have been various attempts to characterize this multipath phenomenon statistically by researchers and it has been found that the statistical nature of the multipath channel gain in PLC is highly site-specific. In many of the studies around the statistical characteristics for PLC channels, it has been found that the envelope of the channel gain follows a Rayleigh distribution in the studies of a) the peak and notch channel transfer function widths in the range of 30 kHz - 100 MHz [8]; b) all the arrival paths of a PLC channel utilizing the NAYY50SE house cable connections for power transfer [9], [10]; and (c) power lines used in the mass transmit systems for trains [11] and other automobile networks. Thus, various researchers consider this channel model for the study and development of novel technologies revolving around PLC [12]–[14].

In addition to the multipath phenomenon, additive noise in PLC systems also leads to unreliable data transmission over the power line channels. The most common type of noise adversely affecting the PLC channels is the additive background noise which arises due to the multiple reflections from the connecting nodes and terminals of the network of the thermal noise emitting by low power consuming loads in the power grid. Statistically this noise has been modeled by a complex Nakagami- m random variable via experimental studies for the range of $m < 1$, and thus this noise model has been extensively used in the literature for various performance studies of PLC systems [13], [15], [16].

There have been numerous studies in the literature to improve the reliability of data transmission in PLC technologies.

Similar to wireless communications, diversity schemes have also been employed in PLC to obtain a better error performance of the system. The authors in [17] and [18] have considered multiple physical wireline channels to improve the reliability of data transmission considering the channels to be statistically correlated. Such kind of correlation among the PLC channels have also been experimentally studied for the case of inductive coupling among wirelines and in houses of North America in [19] and [20], respectively. Furthermore, the authors in [21] and [22] have considered an optimal and a suboptimal receiver, respectively, to obtain closed form expressions of the symbol error probability (SEP) for a receive diversity PLC system corrupted by additive Nakagami- m background noise by employing binary phase-shift keying (BPSK) modulation for data transmission. In addition, the authors in [23] obtain expressions for the outage probability and the bit error probability for a PLC system under correlated background noise, while the authors in [24], and [25] obtain expressions of the SEP for BPSK and quadrature phase-shift keying (QPSK) signaling schemes for suboptimal receivers, respectively, all for single channel PLC systems. There have been attempts by researchers to employ higher modulation schemes and to optimize them for improved reliability in the performance of PLC systems. Some of those studies are carried out by the authors in [26] who have considered the performance of a receive diversity PLC system employing a sub-optimal maximal-ratio combining (MRC) receiver with M -ary phase-shift keying (M -PSK) signaling scheme for data transmission. Moreover, the authors in [27] have obtained the optimal QPSK constellation minimizing the SEP of a receive diversity PLC system under Nakagami- m noise environment.

The work in this paper is quite different from [27] in that we consider a receive diversity PLC system with the multiple channel gains to be correlated with each other. The major contributions of the paper can be summarized as follows:

- Considering the receive diversity channel gains to be statistically following correlated Rayleigh distributions and the noise in the multiple channels to be following the Nakagami- m distributions, we obtain the optimal maximum likelihood (ML) receiver for the system.
- Using this receiver, we obtain a closed form expression of the union bound on SEP of the system employing the 4-ary imbalanced-phase-amplitude modulation (I-PAM) for data transmission.
- An optimization problem is formulated to obtain the optimal 4-ary I-PAM constellation minimizing the obtained SEP and is solved for numerically.
- The optimization leads to the result that the optimal 4-ary I-PAM constellation which leads to the minimum value of the SEP possible for the considered PLC system is elliptical in nature at lower signal-to-noise ratio (SNR) values as opposed to the traditional circular QPSK constellation scheme.
- Furthermore, the dependency of the elliptical nature of the optimal constellation with the number of diversity branches and the correlation coefficient are studied via numerical results.

Thus, the elliptical optimal 4-ary I-PAM constellation outperforms the traditional QPSK constellation, specifically at lower values of SNR in PLC systems employing lower diversity branches for data transmission. Such kind of novel modulation schemes improve the reliability of the PLC systems which need to follow the electromagnetic compatibility by limiting the electromagnetic interference effects, which, in turn, is ensured by the use of lower signal power of the data transmitted through a lower number of power line channels [28]. Furthermore, the optimal constellation obtained can be used with Turbo and low density parity check codes to outperform the uncoded modulation schemes even at lower SNR values [29].

The rest of the paper is organized as follows. Section II describes the system model of the considered PLC system and obtains the expression of the optimal ML receiver. Closed form expressions for the SEP in the union bound sense and the SEP in the asymptotic sense at high SNR for various types of correlation of PLC channel gains are derived in Section III. Section IV formulates and solves the problem of obtaining the optimal 4-ary I-PAM constellation points numerically to minimize the SEP of the system. Numerical results corroborating the analysis are presented in Section V followed by the conclusions of the paper in Section VI.

II. SYSTEM MODEL

A single-input multiple-output PLC system with N diversity branches along with QPSK modulated data transmission and symbol-by-symbol detection at the receiver is considered. Practical implementation of the multiple receive diversity branches is realized by utilizing the live, neutral, and ground power cables simultaneously for data transmission, thus simplifying the receiver and the transmitter structure [21]. Furthermore, we consider that the topology of the powerline network such that the coherence bandwidth of the channel is higher as compared to the maximum bandwidth of the transmitted signal, which implies that the channel in each of the diversity branches can be modeled by a complex channel gain multiplier. Denoting the transmitted symbol by s , the $N \times 1$ complex channel gain vector and the complex additive noise vector by \mathbf{h} , and \mathbf{n} , respectively, the complex baseband received symbol vector is expressed as

$$\mathbf{r} = \mathbf{h} s + \mathbf{n}. \quad (1a)$$

Let

$$\tilde{\mathbf{r}} = \begin{bmatrix} \Re\{\mathbf{r}\} \\ \Im\{\mathbf{r}\} \end{bmatrix} = \begin{bmatrix} \mathbf{r}_x \\ \mathbf{r}_y \end{bmatrix}, \mathbf{H} = \begin{bmatrix} \Re\{\mathbf{h}\} & -\Im\{\mathbf{h}\} \\ \Im\{\mathbf{h}\} & \Re\{\mathbf{h}\} \end{bmatrix} = \begin{bmatrix} \mathbf{h}_x & -\mathbf{h}_y \\ \mathbf{h}_y & \mathbf{h}_x \end{bmatrix},$$

$$\tilde{\mathbf{n}} = \begin{bmatrix} \Re\{\mathbf{n}\} \\ \Im\{\mathbf{n}\} \end{bmatrix} = \begin{bmatrix} \mathbf{n}_x \\ \mathbf{n}_y \end{bmatrix}, \mathbf{s} = \begin{bmatrix} \Re\{s\} \\ \Im\{s\} \end{bmatrix} = \begin{bmatrix} s_x \\ s_y \end{bmatrix},$$

where $\Re\{\cdot\}$ and $\Im\{\cdot\}$ denote the real and the imaginary part operators, respectively. Thus, the received symbol vector in (1a) can be rewritten in a vector-matrix notation as

$$\tilde{\mathbf{r}} = \mathbf{H} \mathbf{s} + \tilde{\mathbf{n}}. \quad (1b)$$

The multiple PLC channels in consideration are subject to Rayleigh fading, implying that the channel gain coefficients are zero mean complex circular Gaussian random variables with $\mathbf{h} \sim \mathcal{CN}(\mathbf{0}_N, \mathbf{K}_h)$, where $\mathbf{K}_h = \mathbb{E}[\mathbf{h}\mathbf{h}^H]$ is the positive definite covariance matrix of \mathbf{h} , $\mathbf{0}_N$ is the $N \times 1$ vector of zeros, and $(\cdot)^H$ and $\mathbb{E}[\cdot]$ denote the conjugate transpose (Hermitian) and expectation operators, respectively.

The channel covariance matrix \mathbf{K}_h under study is considered under these three categories:

- 1) The case of *independent and identically distributed (i.i.d.) channels* corresponds to the case in which sufficient separation is maintained between the physical channels to ensure that there is no correlation between any of the channels during data transmission. Such kind of topology can also be realized by employing sufficient insulation between the multiple power cables which would lead to minimal electromagnetic interference during data transmission [29]. In this case, \mathbf{K}_h is a diagonal matrix with equal diagonal elements. Thus, its element in the i th row and j th column is given by

$$(\mathbf{K}_h)_{ij} = \begin{cases} \sigma_h^2, & \text{if } i = j, \\ 0, & \text{if } i \neq j, \end{cases} \quad i, j = 1, \dots, N; \quad (2)$$

- 2) The case of *uniformly correlated channels* corresponds to the case in which the inductive coupling phenomenon, leading to correlation amongst the channels, has an equal effect for any two given physical PLC channels [19]. Such correlation model also occurs when the insulation between the multiple wires is not sufficient to prevent the electromagnetic interference effects and the spacing between the power cables is uniform. In this case, \mathbf{K}_h is an uniformly correlated matrix and its element in the i th row and j th column is given by

$$(\mathbf{K}_h)_{ij} = \begin{cases} \sigma_h^2, & \text{if } i = j, \\ \sigma_h^2 \epsilon, & \text{if } i \neq j, \end{cases} \quad i, j = 1, \dots, N, \quad (3a)$$

where

$$-\frac{1}{N-1} < \epsilon < 1, \quad \epsilon \neq 0; \quad (3b)$$

- 3) The case of *exponentially correlated channels* also corresponds to the case when the inductive coupling between the power cables is prominent, the insulation between the multiple power cables is insufficient, or the spacing between the power lines is not uniform [18]. Such modeling of the correlation between the PLC channels has also been experimentally found in certain in-home channels of North American houses and reported in [20]. In this case, \mathbf{K}_h follows an exponential correlation matrix and its element in the i th row and j th column is given by

$$(\mathbf{K}_h)_{ij} = \begin{cases} \sigma_h^2, & \text{if } i = j, \\ \sigma_h^2 e^{|i-j|}, & \text{if } i \neq j, \end{cases} \quad i, j = 1, \dots, N, \quad (4a)$$

where

$$-1 < \epsilon < 1, \quad \epsilon \neq 0. \quad (4b)$$

In all of these cases, $\sigma_h^2 = \text{tr}(\mathbf{K}_h)$ denotes the average variance of the complex channel gains of \mathbf{h} . Further, denoting $\lambda_1, \dots, \lambda_N$ to be the N eigenvalues of the normalized covariance matrix \mathbf{K}_h/σ_h^2 , we can note that

- 1) for the case of i.i.d. channels, all the eigenvalues of the normalized covariance matrix bear the value one, i.e., $\lambda_1 = \dots = \lambda_N = 1$,
- 2) for the case of uniformly correlated channels the eigenvalues of the normalized covariance matrix are $1 - \epsilon$ and $1 + (N - 1)\epsilon$, with multiplicities of $N - 1$ and 1 , respectively, i.e., $\lambda_1 = \dots = \lambda_{N-1} = 1 - \epsilon$ and $\lambda_N = 1 + (N - 1)\epsilon$,
- 3) for the case of exponentially correlated channels, all the eigenvalues of the normalized covariance matrix are distinct.

Thus, the eigendecomposition of \mathbf{K}_h results in

$$\mathbf{K}_h = \sigma_h^2 \mathbf{U} \mathbf{\Lambda} \mathbf{U}^H, \quad (5)$$

where \mathbf{U} is a unitary matrix with orthonormal columns which are the eigenvectors of \mathbf{K}_h and $\mathbf{\Lambda} = \text{diag}(\lambda_1, \dots, \lambda_N)$ with each of the $\lambda_k, k = 1, \dots, N$ being an eigenvalue of \mathbf{K}_h . For the case of i.i.d. channel gains, we have $\mathbf{U} = \mathbf{I}_N$. Owing to the statistics of \mathbf{h} , we have

$$\begin{aligned} \mathbf{h}_x &\sim \mathcal{N}(\mathbf{0}, \mathbf{K}_{h_x}); \quad \mathbf{K}_{h_x} = \mathbb{E}[\mathbf{h}_x \mathbf{h}_x^T] = \frac{\sigma_h^2}{2} \mathbf{U} \mathbf{\Lambda} \mathbf{U}^H, \\ \mathbf{h}_y &\sim \mathcal{N}(\mathbf{0}, \mathbf{K}_{h_y}); \quad \mathbf{K}_{h_y} = \mathbb{E}[\mathbf{h}_y \mathbf{h}_y^T] = \frac{\sigma_h^2}{2} \mathbf{U} \mathbf{\Lambda} \mathbf{U}^H, \end{aligned} \quad (6)$$

and $\mathbb{E}[\mathbf{h}_x \mathbf{h}_y^T] = \mathbb{E}[\mathbf{h}_y \mathbf{h}_x^T] = \mathbf{0}_{N \times N}$, where $(\cdot)^T$ denotes the transpose operator.

The additive background noise in the PLC channels, arising due to multiple low power-consuming devices in the power network, is statistically modeled by a complex Nakagami- m noise. Thus, assuming the noise in the multiple channels to be i.i.d. with the noise variance in each of the channels as σ_n^2 , the envelope of each of the elements in \mathbf{n} follows a Nakagami- m distribution with $m \leq 1$. Owing to the statistical properties of such a random distribution, the noise components at each of the receivers can be approximated by the Nakagami- q or Hoyt distribution for the range of values of $m \in [1/2, 1)$. This implies \mathbf{n}_x and \mathbf{n}_y follow independent Gaussian distributions, i.e., $\mathbb{E}[\mathbf{n}_x \mathbf{n}_y^T] = \mathbf{0}_{N \times N}$ and

$$\mathbf{n}_x \sim \mathcal{N}(\mathbf{0}_N, \sigma_x^2 \mathbf{I}_N), \quad \mathbf{n}_y \sim \mathcal{N}(\mathbf{0}_N, \sigma_y^2 \mathbf{I}_N),$$

where \mathbf{I}_N denotes the $N \times N$ identity matrix,

$$\sigma_x^2 = \frac{\sigma_n^2(1+b)}{2}, \quad \sigma_y^2 = \frac{\sigma_n^2(1-b)}{2}, \quad (7a)$$

and

$$b = \sqrt{\frac{1}{m} - 1}, \quad \frac{1}{2} \leq m < 1. \quad (7b)$$

Furthermore, the transmitted symbol s in (1a) belongs to the set of equiprobable 4-ary I-PAM symbols, denoted by S and expressed as

$$S = \{\pm A_x, \pm j A_y\}, \quad A_x, A_y > 0, \quad (8)$$

where $j = \sqrt{-1}$. Thus, the SNR Γ_x of the symbols $\pm A_x$, the SNR Γ_y of the symbols $\pm j A_y$, and the average SNR per symbol

per branch Γ_{av} are given by

$$\Gamma_x = \frac{A_x^2 \sigma_h^2}{\sigma_n^2}, \Gamma_y = \frac{A_y^2 \sigma_h^2}{\sigma_n^2}, \Gamma_{av} = \frac{\Gamma_x + \Gamma_y}{2}. \quad (9)$$

From the statistics of \mathbf{n} , the noise vector $\tilde{\mathbf{n}}$ in (1b) follows a zero mean Gaussian distribution, i.e., $\tilde{\mathbf{n}} \sim \mathcal{N}(\mathbf{0}_{2N}, \Sigma)$, where

$$\Sigma = \begin{bmatrix} \sigma_x^2 \mathbf{I}_N & \mathbf{0}_{N \times N} \\ \mathbf{0}_{N \times N} & \sigma_y^2 \mathbf{I}_N \end{bmatrix}.$$

Therefore, applying the maximum likelihood (ML) rule, the optimal coherent receiver is obtained as

$$\begin{aligned} \hat{s} &= \arg \min_{s \in S} (\tilde{\mathbf{r}} - \mathbf{H}\mathbf{s})^T \Sigma^{-1} (\tilde{\mathbf{r}} - \mathbf{H}\mathbf{s}) \\ &= \arg \max_{s \in S} \mathbf{s}^T \mathbf{v} - \frac{1}{2} \mathbf{s}^T \begin{bmatrix} B_{xx} & B_{xy} \\ B_{xy} & B_{yy} \end{bmatrix} \mathbf{s}, \end{aligned} \quad (10a)$$

where

$$\mathbf{v} = \mathbf{H}^T \Sigma^{-1} \tilde{\mathbf{r}} = \begin{bmatrix} v_x \\ v_y \end{bmatrix} \quad (10b)$$

and

$$\begin{aligned} \begin{bmatrix} B_{xx} & B_{xy} \\ B_{xy} & B_{yy} \end{bmatrix} &= \mathbf{H}^T \Sigma^{-1} \mathbf{H} \\ &= \begin{bmatrix} \sigma_x^{-2} \|\mathbf{h}_x\|^2 + \sigma_y^{-2} \|\mathbf{h}_y\|^2 & (\sigma_y^2 - \sigma_x^2) \mathbf{h}_x^T \mathbf{h}_y \\ (\sigma_y^2 - \sigma_x^2) \mathbf{h}_x^T \mathbf{h}_y & \sigma_x^{-2} \|\mathbf{h}_y\|^2 + \sigma_y^{-2} \|\mathbf{h}_x\|^2 \end{bmatrix}, \end{aligned} \quad (10c)$$

with $\|\cdot\|$ denoting the Euclidean norm.

III. PAIRWISE ERROR PROBABILITIES AND UNION BOUND ON SEP

For the transmission of the i th symbol, the decision variable $D_{s_i}(\mathbf{v})$ can be expressed from (10a) as

$$D_{s_i}(\mathbf{v}) = \mathbf{s}_i^T \mathbf{v} - \frac{1}{2} \mathbf{s}_i^T \begin{bmatrix} B_{xx} & B_{xy} \\ B_{xy} & B_{yy} \end{bmatrix} \mathbf{s}_i, \quad (11)$$

which can be simplified for the four QPSK constellation points

$$\mathbf{s}_1 = \begin{bmatrix} A_x \\ 0 \end{bmatrix}, \mathbf{s}_2 = \begin{bmatrix} 0 \\ A_y \end{bmatrix}, \mathbf{s}_3 = \begin{bmatrix} -A_x \\ 0 \end{bmatrix}, \mathbf{s}_4 = \begin{bmatrix} 0 \\ -A_y \end{bmatrix},$$

using (11) as

$$\begin{aligned} D_{s_1}(\mathbf{v}) &= A_x v_x - \frac{1}{2} A_x^2 B_{xx}, \\ D_{s_2}(\mathbf{v}) &= A_y v_y - \frac{1}{2} A_y^2 B_{yy}, \\ D_{s_3}(\mathbf{v}) &= -A_x v_x - \frac{1}{2} A_x^2 B_{xx}, \\ D_{s_4}(\mathbf{v}) &= -A_y v_y - \frac{1}{2} A_y^2 B_{yy}. \end{aligned} \quad (12)$$

Furthermore, from the statistics of the additive background noise, we have

$$\mathbf{v}_{|\mathbf{h}, \mathbf{s}} \sim \mathcal{N} \left(\begin{bmatrix} B_{xx} & B_{xy} \\ B_{xy} & B_{yy} \end{bmatrix} \begin{bmatrix} s_x \\ s_y \end{bmatrix}, \begin{bmatrix} B_{xx} & B_{xy} \\ B_{xy} & B_{yy} \end{bmatrix} \right),$$

which further implies that

$$A_x v_x \pm A_y v_y |_{\mathbf{h}, \mathbf{s}} \sim \mathcal{N} \left(\begin{aligned} &(A_x B_{xx} \pm A_y B_{xy}) s_x \\ &+ (A_x B_{xy} \pm A_y B_{yy}) s_y, \\ &A_x^2 B_{xx} + A_y^2 B_{yy} \pm 2A_x A_y B_{xy} \end{aligned} \right). \quad (13)$$

Let us denote the pairwise error probability (PEP) between the i th and the j th symbol by $P_{i \rightarrow j}$, which is given, using (10a), as

$$P_{i \rightarrow j} = \Pr(D_{s_j}(\mathbf{v}) > D_{s_i}(\mathbf{v}) | s_i \text{ is transmitted}). \quad (14)$$

Thus, a closed form expression of the union bound on the SEP is obtained from the PEP expressions, as derived in Appendix A, as

$$\begin{aligned} P_{eUB} &= \frac{1}{4} \sum_{i=1}^4 \sum_{j=1, j \neq i}^4 P_{i \rightarrow j} \\ &\approx \frac{2^N (1-b^2)^{N/2} (2\Gamma_{av} - b(\Gamma_x - \Gamma_y))^{-N/2}}{\sqrt{\prod_{k=1}^N \left[\lambda_k + \frac{4(1-b^2+4\Gamma_{av}^2 \lambda_k^2)}{2\Gamma_{av}-b(\Gamma_x-\Gamma_y)} + \frac{4(16\Gamma_{av}^2+\Gamma_x\Gamma_y)\lambda_k}{(2\Gamma_{av}-b(\Gamma_x-\Gamma_y))^2} \right]}} \\ &\quad + \frac{(1-b^2)^{N/2}}{4 \sqrt{\prod_{k=1}^N (\Gamma_x \lambda_k + 1 + b)(\Gamma_x \lambda_k + 1 - b)}} \\ &\quad + \frac{(1-b^2)^{N/2}}{4 \sqrt{\prod_{k=1}^N (\Gamma_y \lambda_k + 1 + b)(\Gamma_y \lambda_k + 1 - b)}}. \end{aligned} \quad (15)$$

For the case of high SNR, the asymptotic expression for the SEP is derived from (15) and is given as

$$P_e |_{\Gamma_{av} \gg 1} \approx \frac{(1-b^2)^{N/2}}{4 \prod_{k=1}^N \lambda_k} \left(\frac{1}{2^{N-2} \Gamma_{av}^N} + \frac{1}{\Gamma_x^N} + \frac{1}{\Gamma_y^N} \right). \quad (16)$$

The expressions in (15) and (16) are used for the results for the case of exponentially correlated channels. We will discuss the corresponding results for the other cases of channel correlation under consideration in the following subsections.

A. Case of i.i.d. channels

For the case of the channels being i.i.d., all the eigenvalues bear equal values of unity. Thus, the expressions for the union bound on SEP and the corresponding high SNR approximation are obtained from (15) and (16) by substituting $\lambda_k = 1, k =$

$1, \dots, N$ as

$$P_{e_{UB},i.i.d.} \approx \frac{2^N (1-b^2)^{N/2} (2\Gamma_{av} - b(\Gamma_x - \Gamma_y))^{-N/2}}{\left[1 + \frac{4(16\Gamma_{av}^2 + \Gamma_x \Gamma_y)}{(2\Gamma_{av} - b(\Gamma_x - \Gamma_y))^2} + \frac{4(1-b^2 + 4\Gamma_{av}^2)}{2\Gamma_{av} - b(\Gamma_x - \Gamma_y)}\right]^{N/2}} + \frac{(1-b^2)^{N/2}}{4(\Gamma_x^2 + 2\Gamma_x + 1 - b^2)^{N/2}} + \frac{(1-b^2)^{N/2}}{4(\Gamma_y^2 + 2\Gamma_y + 1 - b^2)^{N/2}}, \quad (17a)$$

$$P_{e,i.i.d.}|_{\Gamma_{av} \gg 1} \approx \frac{(1-b^2)^{N/2}}{4} \left(\frac{1}{2^{N-2}\Gamma_{av}^N} + \frac{1}{\Gamma_x^N} + \frac{1}{\Gamma_y^N} \right). \quad (17b)$$

B. Case of uniformly correlated channels

For the case of the channels being uniformly correlated, the eigenvalue $1 - \epsilon$ has a multiplicity of $N - 1$ and the eigenvalue $1 + (N - 1)\epsilon$ has a multiplicity of one. Thus, the expressions for the union bound on SEP and the corresponding high SNR approximation are obtained from (15) and (16) as in (18a), shown at the bottom of this page, and (18b)

$$P_{e,uni}|_{\Gamma_{av} \gg 1} \approx \frac{(1-b^2)^{N/2}}{4(1-\epsilon)^{N-1}(1+(N-1)\epsilon)} \times \left(\frac{1}{2^{N-2}\Gamma_{av}^N} + \frac{1}{\Gamma_x^N} + \frac{1}{\Gamma_y^N} \right). \quad (18b)$$

IV. OPTIMAL 4-ARY I-PAM CONSTELLATION PARAMETERS

The optimal values of the 4-ary I-PAM parameters Γ_x and Γ_y are derived to obtain the minimum SEP for the PLC system under the constraint of constant average transmit power. Equivalently, using (15), the optimization problem at hand can be formulated

as

$$\min_{\substack{\Gamma_x, \Gamma_y \\ \Gamma_x + \Gamma_y = 2\Gamma_{av}}} P_{e_{UB}}. \quad (19)$$

Although the optimization problem proposed in (19) is not being proven to be convex herein, it can be observed that for the asymptotic expression of the SEP given in (16) that the formulated optimization is convex in nature. Thus, to utilize the Lagrangian multiplier technique for solving the optimization problem, the modified objective function is given by

$$G(\Gamma_x, \Gamma_y, \lambda) = P_{e_{UB}} + \lambda(\Gamma_x + \Gamma_y - 2\Gamma_{av}). \quad (20)$$

The optimal values of the 4-ary I-PAM constellation parameters, denoted by $\Gamma_{x,opt}$ and $\Gamma_{y,opt}$ are obtained by solving the set of equations expressed as

$$\frac{\partial G(\Gamma_x, \Gamma_y, \lambda)}{\partial \Gamma_x} = 0, \quad \frac{\partial G(\Gamma_x, \Gamma_y, \lambda)}{\partial \Gamma_y} = 0, \quad \frac{\partial G(\Gamma_x, \Gamma_y, \lambda)}{\partial \lambda} = 0, \quad (21)$$

which can be further simplified by some algebra as

$$\left[\begin{array}{l} \sum_{j=1}^N \frac{\lambda_j (1 + \Gamma_y \lambda_j) (1 - b^2 + 2\Gamma_x \lambda_j + \Gamma_x^2 \lambda_j^2)^{-3/2}}{2 \sqrt{\prod_{\substack{k=1 \\ k \neq j}}^N (1 - b^2 + 2\Gamma_x \lambda_k + \Gamma_x^2 \lambda_k^2)}} \\ \\ - \frac{\lambda_j (1 + \Gamma_y \lambda_j) (1 - b^2 + 2\Gamma_y \lambda_j + \Gamma_y^2 \lambda_j^2)^{-3/2}}{2 \sqrt{\prod_{\substack{k=1 \\ k \neq j}}^N (1 - b^2 + 2\Gamma_y \lambda_k + \Gamma_y^2 \lambda_k^2)}} \end{array} \right]$$

$$P_{e_{UB},uni} \approx \frac{2^N (1-b^2)^{N/2} (2\Gamma_{av} - b(\Gamma_x - \Gamma_y))^{-N/2}}{\sqrt{\left[(1-\epsilon) + \frac{4(1-b^2 + 4\Gamma_{av}^2(1-\epsilon)^2)}{2\Gamma_{av} - b(\Gamma_x - \Gamma_y)} + \frac{4(16\Gamma_{av}^2 + \Gamma_x \Gamma_y)(1-\epsilon)}{(2\Gamma_{av} - b(\Gamma_x - \Gamma_y))^2} \right]^{N-1}}} \times \frac{1}{\sqrt{\left[(1+(N-1)\epsilon) + \frac{4(1-b^2 + 4\Gamma_{av}^2(1+(N-1)\epsilon)^2)}{2\Gamma_{av} - b(\Gamma_x - \Gamma_y)} + \frac{4(16\Gamma_{av}^2 + \Gamma_x \Gamma_y)(1+(N-1)\epsilon)}{(2\Gamma_{av} - b(\Gamma_x - \Gamma_y))^2} \right]}}} + \frac{(1-b^2)^{N/2} ((1-\epsilon)\Gamma_x^2 + 2(1-\epsilon)\Gamma_x + 1 - b^2)^{-(N-1)/2}}{4\sqrt{(1+(N-1)\epsilon)\Gamma_x^2 + 2(1+(N-1)\epsilon)\Gamma_x + 1 - b^2}} + \frac{(1-b^2)^{N/2} ((1-\epsilon)\Gamma_y^2 + 2(1-\epsilon)\Gamma_y + 1 - b^2)^{-(N-1)/2}}{4\sqrt{(1+(N-1)\epsilon)\Gamma_y^2 + 2(1+(N-1)\epsilon)\Gamma_y + 1 - b^2}} \quad (18a)$$

$$\begin{aligned}
&= \sum_{j=1}^N \frac{2^{N+1} \left[b\lambda_j + \frac{2(\Gamma_x - \Gamma_y)\lambda_j}{2\Gamma_{av} - b(\Gamma_x - \Gamma_y)} - \frac{4b(16\Gamma_{av}^2 + \Gamma_x\Gamma_y)\lambda_j}{(2\Gamma_{av} - b(\Gamma_x - \Gamma_y))^2} \right]}{\sqrt{\left[\lambda_j + \frac{4(1-b^2+4\Gamma_{av}^2\lambda_j^2)}{2\Gamma_{av} - b(\Gamma_x - \Gamma_y)} + \frac{4(16\Gamma_{av}^2 + \Gamma_x\Gamma_y)\lambda_j}{(2\Gamma_{av} - b(\Gamma_x - \Gamma_y))^2} \right]^3}} \\
&\times \frac{(2\Gamma_{av} - b(\Gamma_x - \Gamma_y))^{-(N+2)/2}}{\sqrt{\prod_{\substack{k=1 \\ k \neq j}}^N \left[\lambda_k + \frac{4(1-b^2+4\Gamma_{av}^2\lambda_k^2)}{2\Gamma_{av} - b(\Gamma_x - \Gamma_y)} + \frac{4(16\Gamma_{av}^2 + \Gamma_x\Gamma_y)\lambda_k}{(2\Gamma_{av} - b(\Gamma_x - \Gamma_y))^2} \right]}}, \quad (22a)
\end{aligned}$$

and

$$\Gamma_x + \Gamma_y = 2\Gamma_{av}. \quad (22b)$$

By solving the set of expressions in (22a) and (22b) numerically, we obtain the optimal solutions for the parameters of the 4-ary I-PAM constellation used for symbol transmission. In the following subsection, we discuss analytical results for $\Gamma_{x,opt}$ and $\Gamma_{y,opt}$ for the asymptotic case of high SNR.

A. Asymptotic Results

For the case of high SNR, the optimization problem, equivalent to (19), can be formulated as

$$\begin{aligned}
\min_{\Gamma_x, \Gamma_y} \quad & P_e |_{\Gamma_{av} \gg 1}, \quad (23) \\
\Gamma_x + \Gamma_y = & 2\Gamma_{av}
\end{aligned}$$

and the corresponding modified objective function using the Lagrangian multiplier technique is obtained as

$$H(\Gamma_x, \Gamma_y, \lambda) = P_e |_{\Gamma_{av} \gg 1} + \lambda(\Gamma_x + \Gamma_y - 2\Gamma_{av}). \quad (24)$$

Thus, the optimal values of the 4-ary I-PAM constellation parameters, $\Gamma_{x,opt}$ and $\Gamma_{y,opt}$, are obtained by solving the set of equations expressed as

$$\frac{\partial H(\Gamma_x, \Gamma_y, \lambda)}{\partial \Gamma_x} = 0, \quad \frac{\partial H(\Gamma_x, \Gamma_y, \lambda)}{\partial \Gamma_y} = 0, \quad \frac{\partial H(\Gamma_x, \Gamma_y, \lambda)}{\partial \lambda} = 0, \quad (25)$$

From the symmetry of the asymptotic expression of the SEP in (16) and using some algebra in (25), it can be observed that the optimal 4-ary I-PAM constellation parameters for the case of high SNR are obtained as

$$\Gamma_{x,opt} = \Gamma_{y,opt} = \Gamma_{av}. \quad (26)$$

Therefore, the optimal asymptotic expression for the SEP at high SNR, denoted by $P_{e,opt} |_{\Gamma_{av} \gg 1}$, is obtained as

$$P_{e,opt} |_{\Gamma_{av} \gg 1} = \frac{(2^{N-1} + 1)(1 - b^2)^{N/2}}{2^N \Gamma_{av}^N \prod_{k=1}^N \lambda_k}, \quad (27)$$

which can be further simplified for the specific cases of channel correlations as

$$P_{e,i.i.d.,opt} |_{\Gamma_{av} \gg 1} = \frac{(2^{N-1} + 1)(1 - b^2)^{N/2}}{2^N \Gamma_{av}^N}, \quad (28a)$$

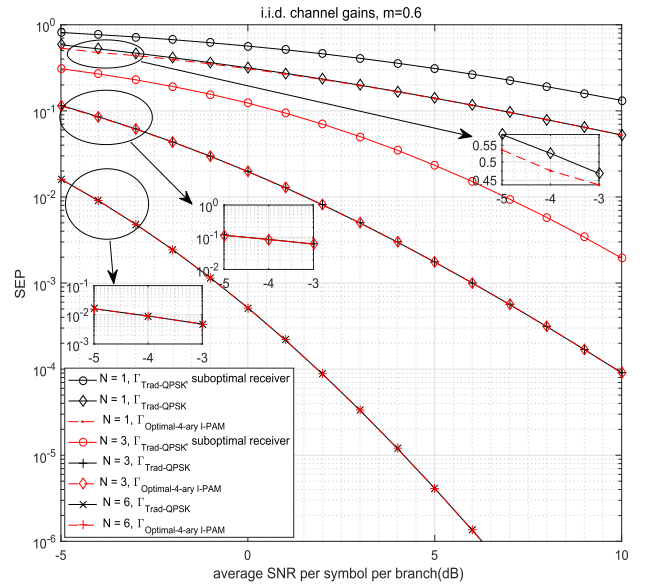


Fig. 1. SEP versus the average SNR per symbol per branch with traditional QPSK and optimal 4-ary I-PAM constellations for i.i.d. channel gains, $N = 1, 3, 6$, and $m = 0.6$.

and

$$P_{e,uni,opt} |_{\Gamma_{av} \gg 1} = \frac{(2^{N-1} + 1)(1 - b^2)^{N/2}}{2^N (1 - \epsilon)^{N-1} (1 + (N-1)\epsilon) \Gamma_{av}^N}. \quad (28b)$$

It is to be noted from (16) and (27) that the PLC system under consideration achieves full diversity. Thus, the optimal values of the constellation parameters do not improve the diversity of the system, however, they improve the error performance of the system. It is also to be noted that the diversity order of the PLC system is independent of the shape parameter m of the noise.

V. NUMERICAL RESULTS

This section presents the numerical study of the performance metric of the system under consideration with the variations in the system parameters. For all the plots presented, the notation “Trad-QPSK” refers to the traditional circular QPSK constellation used in communication systems and “Optimal-QPSK” refers to the optimal 4-ary I-PAM constellation minimizing the SEP for the PLC system in study. The SEP versus the average SNR per symbol per branch for the PLC system with i.i.d. channel gains and for varying values of number of diversity branches N with traditional QPSK and optimal 4-ary I-PAM constellations is presented in Fig. 1. It is observed that the difference between the performance of the two constellations becomes less prominent with the increase in the number of receive diversity branches and with increase in the values of SNR. This implies that the optimal QPSK constellation obtained has practical utility to reduce the system error probability for the PLC system at lower SNR values. It is also observed that the performance of the optimal receiver employing optimal QPSK constellation for data transmission outperforms the performance of the suboptimal receiver’s performance as given in [26]. Fig. 2

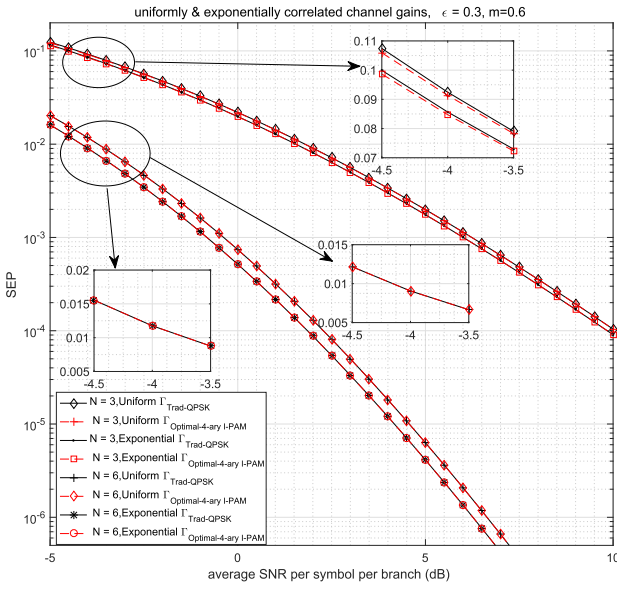


Fig. 2. SEP versus the average SNR per symbol per branch with traditional QPSK and optimal 4-ary I-PAM constellations for uniformly and exponentially correlated channel gains, $\epsilon = 0.3$, $N = 1, 3, 6$, and $m = 0.6$.

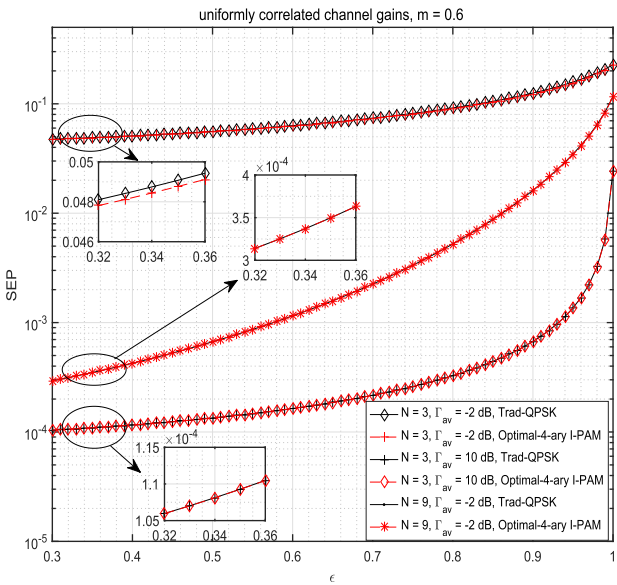


Fig. 3. SEP versus correlation coefficient with traditional QPSK and optimal 4-ary I-PAM constellations for uniformly correlated channel gains, $N = 3, 9$, $\Gamma_{\text{av}} = -2, 10$ dB, and $m = 0.6$.

presents the comparative study of the SEP of the PLC system versus the average SNR per symbol per branch with the channels being uniformly and exponentially correlated and for the QPSK constellation taking the traditional and the optimal values. It is observed that for a given value of the correlation coefficient ϵ and the shape parameter m of the noise, the difference between the superior performance of exponential correlation over uniform correlation is more prominent with increase in the number of diversity branches. Further, as in the earlier case, it is observed that the effect of optimality of the QPSK constellation is related

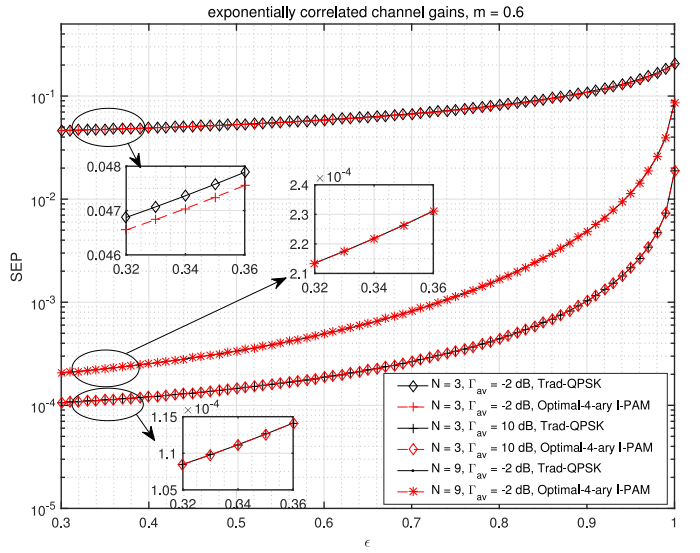


Fig. 4. SEP versus correlation coefficient with traditional QPSK and optimal 4-ary I-PAM constellations for exponentially correlated channel gains, $N = 3, 9$, $\Gamma_{\text{av}} = -2, 10$ dB, and $m = 0.6$.

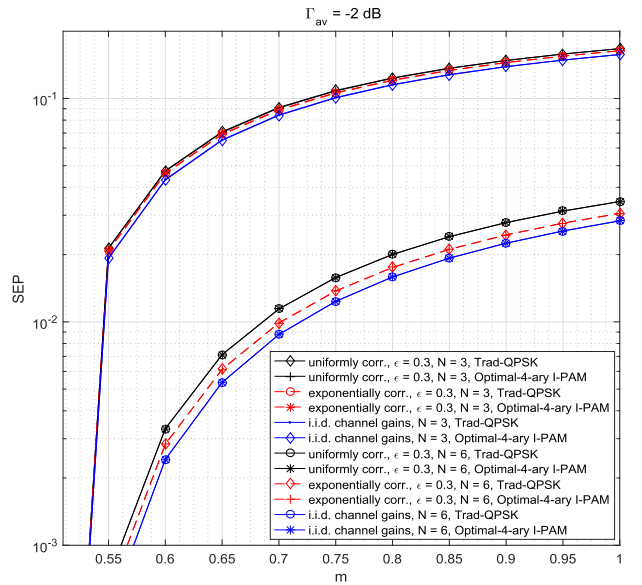


Fig. 5. SEP versus the shape parameter of noise with traditional QPSK and optimal 4-ary I-PAM constellations for i.i.d., uniformly, and exponentially correlated channel gains, $\epsilon = 0.3, 0.7$, $N = 3, 6$, and $\Gamma_{\text{av}} = -2$ dB.

at lower SNR values and for lower diversity branches. The plots of the variation of the SEP of the system with respect to the correlation coefficient ϵ for a given value of m with varying SNR values, number of diversity branches N , and for the traditional and optimal 4-ary I-PAM constellations are presented in Fig. 3 and Fig. 4 for the channel gains being uniformly correlated and exponentially correlated, respectively. It is observed that the optimal QPSK constellation outperforms the traditional QPSK constellation and the difference in the performance is prominent at lower values of the correlation coefficient ϵ and for the case of exponentially correlated channel gains as compared to the

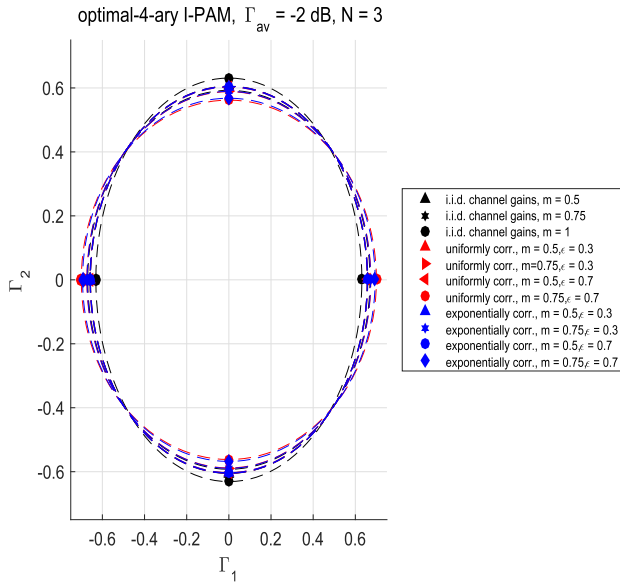


Fig. 6. Optimal constellation plot for 4-ary I-PAM scheme for i.i.d., uniformly, and exponentially correlated channel gains, $\epsilon = 0.3, 0.7$, $N = 3$, $m = 0.5, 0.75, 1$, and $\Gamma_{av} = -2$ dB.

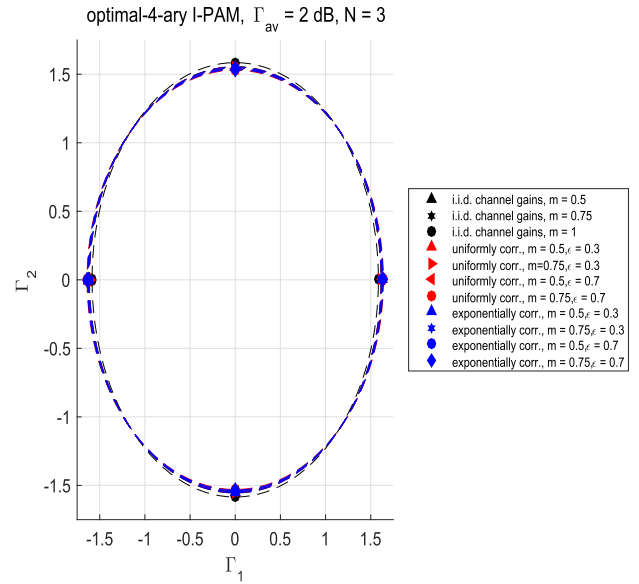


Fig. 8. Optimal constellation plot for 4-ary I-PAM scheme for i.i.d., uniformly, and exponentially correlated channel gains, $\epsilon = 0.3, 0.7$, $N = 3$, $m = 0.5, 0.75, 1$, and $\Gamma_{av} = 2$ dB.

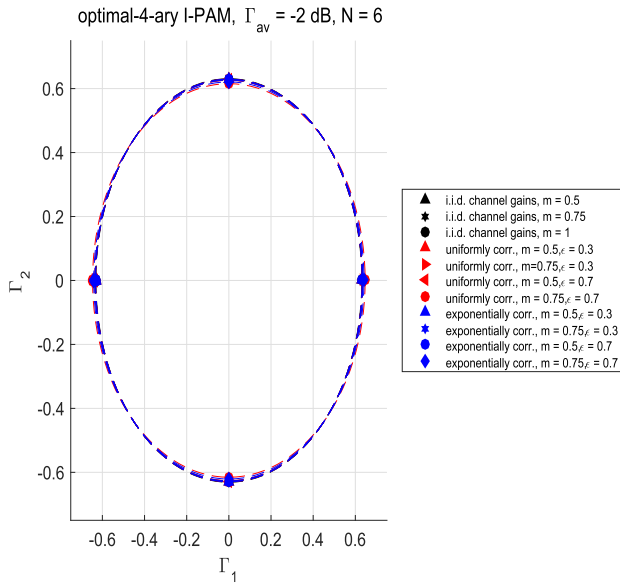


Fig. 7. Optimal constellation plot for 4-ary I-PAM scheme for i.i.d., uniformly, and exponentially correlated channel gains, $\epsilon = 0.3, 0.7$, $N = 6$, $m = 0.5, 0.75, 1$, and $\Gamma_{av} = -2$ dB.

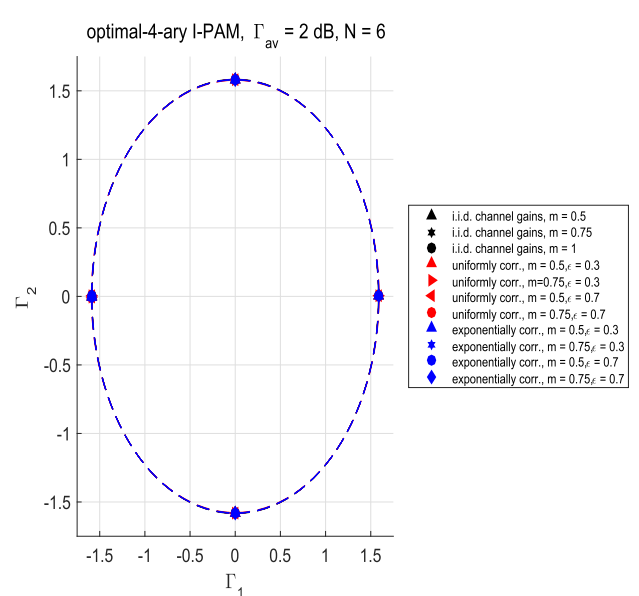


Fig. 9. Optimal constellation plot for 4-ary I-PAM scheme for i.i.d., uniformly, and exponentially correlated channel gains, $\epsilon = 0.3, 0.7$, $N = 6$, $m = 0.5, 0.75, 1$, and $\Gamma_{av} = 2$ dB.

uniformly correlated channel gains. Fig. 5 presents the variation of the SEP performance of the system versus the shape parameter m of the noise for other varying system parameters. Along with the similar trends obtained earlier, it is also observed that the effect of m on the performance of the system is more prominent at higher values of m and for the PLC systems employing higher receive diversity branches. Thus, the correlation among the diversity branches has negligible effect on the performance of the system provided the shape parameter of the noise is smaller in value. It is also observed that the performance of the optimal

and the traditional QPSK is almost independent of the shape parameter m of the noise. However, the variation of the optimal constellation itself with respect to the shape parameter is not very clear and is therefore, studied next. The optimal 4-ary I-PAM constellation plots for the average SNR per symbol per branch, $\Gamma_{av} = -2$ dB with the number of receive diversity branches as $N = 3$ for varying values of m and ϵ and for i.i.d. and correlated channel gains are presented in Fig. 6. It is observed that the optimal 4-ary I-PAM constellation becomes elliptical in shape

with the increase in the correlation among the channel gains. Furthermore, the optimal 4-ary I-PAM constellation is significantly elliptical for uniformly correlated channel gains as compared to exponentially correlated gains and i.i.d. channel gains. It is also observed that the elliptical nature of the constellation is prominent for lower values of the noise shape parameter m and is identical to the traditional QPSK constellation for $m = 1$, for which the Nakagami- m random noise becomes equivalent to the additive white Gaussian noise. Similar variations of the optimal 4-ary I-PAM constellations for various values of the average SNR per symbol per branch and number of receive diversity branches with the correlation of the channel gains and values of the shape parameter of the noise are studied in Figs. 7, 8, and 9. In addition to the similar trend as in the previous case, it is observed that the distinction between the optimal and the traditional QPSK constellations becomes negligible with the increase in SNR values and in the number of diversity branches, which is in line of the previous numerical and computational observations.

VI. CONCLUSION

We consider an N -branch receive diversity PLC system with the multiple branches being exponentially correlated, uniformly correlated, and uncorrelated, and the additive Nakagami- m background noise affecting the reliability of data transmission over the PLC medium. The optimal receiver is derived, using which the union bound expression and the asymptotic expression for the SEP are obtained for the PLC system employing QPSK modulation for data signaling. The optimization problem to minimize the obtained SEP under the constraint of total average energy is formulated and solved numerically to arrive at the optimal 4-ary I-PAM constellation. It is observed that the optimal 4-ary I-PAM constellation thus obtained follows an elliptical diagram when compared to the circular QPSK constellation utilized in traditional wireless communication systems. It is further observed that the ellipticity of the constellation tends to the circular constellation with increase in the average SNR per symbol per branch, the number of diversity branches, and the correlation coefficient among the diversity branches and with the value of the shape parameter of the additive complex noise. This provides us practical design parameters to choose from, for various choices of the system parameters at hand.

APPENDIX

DERIVATION OF THE EXPRESSION OF PEP (15)

Owing to the statistics of \mathbf{n} , and from (12), (13), and (14), the conditional PEP, conditioned on the channel vector \mathbf{h} , between \mathbf{s}_1 and \mathbf{s}_2 can be expressed as

$$\begin{aligned} P_{1 \rightarrow 2} |_{\mathbf{h}} &= \Pr \left(A_y v_y - A_x v_x > \frac{1}{2} (A_y^2 B_{yy} - A_x^2 B_{xx}) \mid \mathbf{s}_1 \right) \\ &= Q \left(\frac{1}{2} \sqrt{A_x^2 B_{xx} + A_y^2 B_{yy} - 2A_x A_y B_{xy}} \right), \quad (29) \end{aligned}$$

where $Q(\cdot)$ denotes the Gaussian- Q function. Using the approximation $Q(x) \approx \exp\{-x^2/2\}/2$ and utilizing (10c) followed by

some algebra, the expression in (29) can be rewritten as

$$\begin{aligned} P_{1 \rightarrow 2} |_{\mathbf{h}} &= \frac{1}{2} \exp \left\{ -\frac{A_x^2 \sigma_x^{-2} + A_y^2 \sigma_y^{-2}}{8} \left\| \mathbf{h}_x - \frac{A_x A_y (\sigma_y^{-2} - \sigma_x^{-2})}{A_x^2 \sigma_x^{-2} + A_y^2 \sigma_y^{-2}} \mathbf{h}_y \right\|^2 \right\} \\ &\times \exp \left\{ -\frac{(A_x^2 + A_y^2) \sigma_x^{-2} \sigma_y^{-2} \|\mathbf{h}_y\|^2}{8 (A_x^2 \sigma_x^{-2} + A_y^2 \sigma_y^{-2})} \right\}. \quad (30) \end{aligned}$$

From the statistics of \mathbf{h} in (6), we have

$$\begin{aligned} \mathbf{u} &\triangleq \mathbf{h}_x - \frac{A_x A_y (\sigma_y^{-2} - \sigma_x^{-2})}{A_x^2 \sigma_x^{-2} + A_y^2 \sigma_y^{-2}} \mathbf{h}_y \Big|_{\mathbf{h}_y} \\ &\sim \mathcal{N} \left(-\frac{A_x A_y (\sigma_y^{-2} - \sigma_x^{-2})}{A_x^2 \sigma_x^{-2} + A_y^2 \sigma_y^{-2}} \mathbf{h}_y, \frac{\mathbf{K}_h}{2} \right), \end{aligned}$$

which further implies that the conditional characteristic function (c.f.) of \mathbf{u} , conditioned on \mathbf{h}_y , is given as

$$\Psi_{\mathbf{u} | \mathbf{h}_y} (j\omega) = \frac{\exp \left\{ \frac{j\omega A_x^2 A_y^2 (\sigma_y^{-2} - \sigma_x^{-2})^2}{(A_x^2 \sigma_x^{-2} + A_y^2 \sigma_y^{-2})^2} \sum_{k=1}^N \frac{\tilde{\mu}_k}{1 - j\omega \sigma_h^2 \lambda_k} \right\}}{\sqrt{\prod_{k=1}^N (1 - j\omega \sigma_h^2 \lambda_k)}}, \quad (31)$$

where $\tilde{\mu} = \mathbf{U}^T \mathbf{h}_y$, and \mathbf{U} and Λ are given by (5). Utilizing (31) in (30) followed by some algebra leads to the conditional expression of the PEP conditioned on \mathbf{h}_y , which is given by

$$P_{1 \rightarrow 2} |_{\mathbf{h}_y} = \frac{2^{\frac{3N}{2}-1} \exp \left\{ -\tilde{\mu}^T \tilde{\Lambda} \tilde{\mu} \right\}}{\sqrt{\prod_{k=1}^N [8 + (A_x^2 \sigma_x^{-2} + A_y^2 \sigma_y^{-2}) \sigma_h^2 \lambda_k]}}, \quad (32a)$$

where $\tilde{\Lambda} = \text{diag}(\tilde{\lambda}_1, \dots, \tilde{\lambda}_N)$ and

$$\begin{aligned} \tilde{\lambda}_k &= \frac{(A_x^2 + A_y^2)^2 \sigma_x^{-2} \sigma_y^{-2} + \frac{8A_x^2 A_y^2 (\sigma_y^{-2} - \sigma_x^{-2})^2}{8 + (A_x^2 \sigma_x^{-2} + A_y^2 \sigma_y^{-2}) \sigma_h^2 \lambda_k}}{8 (A_x^2 \sigma_x^{-2} + A_y^2 \sigma_y^{-2})} \\ &k = 1, \dots, N. \quad (32b) \end{aligned}$$

From the statistics of \mathbf{h}_y given in (6), it is observed that $\tilde{\mu} \sim \mathcal{N}(\mathbf{0}_N, (\sigma_h^2/2)\Lambda)$, and thus the c.f. of $\tilde{\mu}^T \tilde{\Lambda} \tilde{\mu}$ is obtained as

$$\Psi_{\tilde{\mu}^T \tilde{\Lambda} \tilde{\mu}} (j\omega) = \frac{1}{\prod_{k=1}^N (1 - j\omega \tilde{\lambda}_k \lambda_k)}. \quad (33)$$

Furthermore, using (33) and (9) in (32a) to un-condition on \mathbf{h}_y leads to the expression of the PEP between \mathbf{s}_1 and \mathbf{s}_2 , which is given as

$$\begin{aligned} P_{1 \rightarrow 2} &\approx \frac{2^{N-1} (1 - b^2)^{N/2} (2\Gamma_{av} - b(\Gamma_x - \Gamma_y))^{-N/2}}{\sqrt{\prod_{k=1}^N \left[\lambda_k + \frac{4(1-b^2+4\Gamma_{av}^2 \lambda_k^2)}{2\Gamma_{av}-b(\Gamma_x-\Gamma_y)} + \frac{4(16\Gamma_{av}^2+\Gamma_x\Gamma_y)\lambda_k}{(2\Gamma_{av}-b(\Gamma_x-\Gamma_y))^2} \right]}}. \quad (34) \end{aligned}$$

Similarly, owing to the statistics of \mathbf{n} , and from (12), (13), and (14), the conditional PEP, conditioned on the channel vector \mathbf{h} ,

between \mathbf{s}_1 and \mathbf{s}_3 can be expressed as

$$\begin{aligned} P_{1 \rightarrow 3} |_{\mathbf{h}} &= \Pr(v_x < 0 | \mathbf{s}_1) \\ &= Q\left(\sqrt{A_x^2 B_{xx}}\right). \end{aligned} \quad (35)$$

Furthermore, from the statistics of \mathbf{h}_x and \mathbf{h}_y in (6), the c.f.s of $\|\mathbf{h}_x\|^2$ and $\|\mathbf{h}_y\|^2$ are obtained as

$$\Psi_{\|\mathbf{h}_x\|^2}(j\omega) = \Psi_{\|\mathbf{h}_y\|^2}(j\omega) = \frac{1}{\sqrt{\prod_{k=1}^N (1 - j\omega\sigma_h^2\lambda_k)}}. \quad (36)$$

Using the approximation $Q(x) \approx \exp\{-x^2/2\}/2$ and utilizing (10c), (36), and (9) along with the statistical independence of \mathbf{h}_x and \mathbf{h}_y followed by some algebra, the PEP expression in (35) can be obtained as

$$\begin{aligned} P_{1 \rightarrow 3} &\approx \frac{1}{2} \mathbb{E}_{\|\mathbf{h}_x\|^2} \left[\exp\left\{-\frac{A_x^2\sigma_x^{-2}\|\mathbf{h}_x\|^2}{2}\right\} \right] \\ &\quad \times \mathbb{E}_{\|\mathbf{h}_y\|^2} \left[\exp\left\{-\frac{A_y^2\sigma_y^{-2}\|\mathbf{h}_y\|^2}{2}\right\} \right] \\ &= \frac{(1-b^2)^{N/2}}{2\sqrt{\prod_{k=1}^N (\Gamma_x\lambda_k + 1 + b)(\Gamma_x\lambda_k + 1 - b)}}. \end{aligned} \quad (37)$$

Furthermore, from the statistics of \mathbf{n} , and from (12), (13), and (14), the conditional PEP, conditioned on the channel vector \mathbf{h} , between \mathbf{s}_1 and \mathbf{s}_4 can be expressed as

$$\begin{aligned} P_{1 \rightarrow 4} |_{\mathbf{h}} &= \Pr\left(-A_x v_x - A_y v_y > \frac{1}{2}(A_y^2 B_{yy} - A_x^2 B_{xx}) \mid \mathbf{s}_1\right) \\ &= Q\left(\frac{1}{2}\sqrt{A_x^2 B_{xx} + A_y^2 B_{yy} + 2A_x A_y B_{xy}}\right). \end{aligned} \quad (38a)$$

It is observed that the expression in (38a) is similar to the expression of the conditional PEP in (29) with A_y being replaced with $-A_y$. Thus, using similar steps as that from (29) to (34), we have

$$P_{1 \rightarrow 4} = P_{1 \rightarrow 2}. \quad (38b)$$

Along similar lines, the PEP between \mathbf{s}_2 and \mathbf{s}_1 is given by

$$\begin{aligned} P_{2 \rightarrow 1} &= \Pr\left(A_x v_x - A_y v_y > \frac{1}{2}(A_x^2 B_{xx} - A_y^2 B_{yy}) \mid \mathbf{s}_2\right) \\ &= \mathbb{E}_{\mathbf{h}} \left[Q\left(\frac{1}{2}\sqrt{A_x^2 B_{xx} + A_y^2 B_{yy} - 2A_x A_y B_{xy}}\right) \right] \\ &= P_{1 \rightarrow 2}, \end{aligned} \quad (39)$$

the PEP between \mathbf{s}_2 and \mathbf{s}_3 is given by

$$\begin{aligned} P_{2 \rightarrow 3} &= \Pr\left(-A_x v_x - A_y v_y > \frac{1}{2}(A_x^2 B_{xx} - A_y^2 B_{yy}) \mid \mathbf{s}_2\right) \\ &= \mathbb{E}_{\mathbf{h}} \left[Q\left(\frac{1}{2}\sqrt{A_x^2 B_{xx} + A_y^2 B_{yy} + 2A_x A_y B_{xy}}\right) \right] \\ &= P_{1 \rightarrow 4}, \end{aligned} \quad (40)$$

and the PEP between \mathbf{s}_2 and \mathbf{s}_4 is obtained as

$$\begin{aligned} P_{2 \rightarrow 4} &= \Pr(v_y < 0 | \mathbf{s}_2) \\ &= \mathbb{E}_{\mathbf{h}} \left[Q\left(\sqrt{A_y^2 B_{yy}}\right) \right] \\ &\approx \frac{1}{2} \mathbb{E}_{\|\mathbf{h}_x\|^2} \left[\exp\left\{-\frac{A_y^2\sigma_y^{-2}\|\mathbf{h}_x\|^2}{2}\right\} \right] \\ &\quad \times \mathbb{E}_{\|\mathbf{h}_y\|^2} \left[\exp\left\{-\frac{A_y^2\sigma_x^{-2}\|\mathbf{h}_y\|^2}{2}\right\} \right] \\ &= \frac{(1-b^2)^{N/2}}{2\sqrt{\prod_{k=1}^N (\Gamma_y\lambda_k + 1 + b)(\Gamma_y\lambda_k + 1 - b)}}, \end{aligned} \quad (41)$$

where (41) is obtained by utilizing the approximation $Q(x) \approx \exp\{-x^2/2\}/2$ along with (10c), (36), and (9), and the statistical independence of \mathbf{h}_x and \mathbf{h}_y followed by some algebra.

Furthermore, the PEP between \mathbf{s}_3 and \mathbf{s}_1 is given by

$$\begin{aligned} P_{3 \rightarrow 1} &= \Pr(v_x > 0 | \mathbf{s}_3) \\ &= \mathbb{E}_{\mathbf{h}} \left[Q\left(\sqrt{A_x^2 B_{xx}}\right) \right] \\ &= P_{1 \rightarrow 3}, \end{aligned} \quad (42)$$

the PEP between \mathbf{s}_3 and \mathbf{s}_2 is given by

$$\begin{aligned} P_{3 \rightarrow 2} &= \Pr\left(A_x v_x + A_y v_y > \frac{1}{2}(A_y^2 B_{yy} - A_x^2 B_{xx}) \mid \mathbf{s}_3\right) \\ &= \mathbb{E}_{\mathbf{h}} \left[Q\left(\frac{1}{2}\sqrt{A_x^2 B_{xx} + A_y^2 B_{yy} + 2A_x A_y B_{xy}}\right) \right] \\ &= P_{1 \rightarrow 2}, \end{aligned} \quad (43)$$

the PEP between \mathbf{s}_3 and \mathbf{s}_4 is given by

$$\begin{aligned} P_{3 \rightarrow 4} &= \Pr\left(A_x v_x - A_y v_y > \frac{1}{2}(A_y^2 B_{yy} - A_x^2 B_{xx}) \mid \mathbf{s}_3\right) \\ &= \mathbb{E}_{\mathbf{h}} \left[Q\left(\frac{1}{2}\sqrt{A_x^2 B_{xx} + A_y^2 B_{yy} - 2A_x A_y B_{xy}}\right) \right] \\ &= P_{1 \rightarrow 2}, \end{aligned} \quad (44)$$

the PEP between \mathbf{s}_4 and \mathbf{s}_1 is given by

$$\begin{aligned} P_{4 \rightarrow 1} &= \Pr\left(A_x v_x + A_y v_y > \frac{1}{2}(A_x^2 B_{xx} - A_y^2 B_{yy}) \mid \mathbf{s}_4\right) \\ &= \mathbb{E}_{\mathbf{h}} \left[Q\left(\frac{1}{2}\sqrt{A_x^2 B_{xx} + A_y^2 B_{yy} + 2A_x A_y B_{xy}}\right) \right] \\ &= P_{1 \rightarrow 2}, \end{aligned} \quad (45)$$

the PEP between \mathbf{s}_4 and \mathbf{s}_2 is given by

$$\begin{aligned} P_{4 \rightarrow 2} &= \Pr(v_y > 0 | \mathbf{s}_4) \\ &= \mathbb{E}_{\mathbf{h}} \left[Q\left(\sqrt{A_y^2 B_{yy}}\right) \right] \\ &= P_{2 \rightarrow 4}, \end{aligned} \quad (46)$$

and the PEP between \mathbf{s}_4 and \mathbf{s}_3 is given by

$$\begin{aligned} P_{4 \rightarrow 3} &= \Pr \left(A_y v_y - A_x v_x > \frac{1}{2} (A_x^2 B_{xx} - A_y^2 B_{yy}) \middle| \mathbf{s}_4 \right) \\ &= \mathbb{E}_{\mathbf{h}} \left[Q \left(\frac{1}{2} \sqrt{A_x^2 B_{xx} + A_y^2 B_{yy} - 2A_x A_y B_{xy}} \right) \right] \\ &= P_{1 \rightarrow 2}, \end{aligned} \quad (47)$$

The expressions of the PEPs derived herein are utilized to obtain the expression of an upper bound on the SEP as given in (15).

REFERENCES

- [1] H. C. Ferreira, L. Lampe, J. Newbury, and T. G. Swart, *Power Line Communications: Theory and Applications for Narrowband and Broadband Communications Over Power Lines*, Singapore: Wiley, 2010.
- [2] G. López *et al.*, "The role of power line communications in the smart grid revisited: Applications, challenges, and research initiatives," *IEEE Access*, vol. 7, pp. 117346–117368, Jul. 2019.
- [3] S. P. Dash and S. Joshi, "Cooperative device-to-device relaying network with power line communications," in *Proc. IEEE 90th Veh. Technol. Conf.*, Honolulu, HI, USA, Sep. 2019, pp. 1–5.
- [4] S. P. Dash, S. Joshi, and R. K. Mallik, "Smart grid network with D2D communication and coherent PLC: Error analysis," *IEEE Trans. Veh. Technol.*, vol. 69, no. 1, pp. 1051–1054, Jan. 2020.
- [5] S. P. Dash and S. Joshi, "Performance analysis of a cooperative D2D communication network with NOMA," *IET Commun.*, vol. 14, no. 16, pp. 2731–2739, Oct. 2020.
- [6] S. P. Dash, R. K. Mallik, and S. K. Mohammed, "Error analysis of receive diversity noncoherent PLC system in impulsive noise environment," *IEEE Trans. Veh. Technol.*, vol. 68, no. 1, pp. 962–966, Jan. 2019.
- [7] S. P. Dash, R. K. Mallik, and S. K. Mohammed, "Performance analysis of noncoherent PLC with multi-level ASK in impulsive noise environment," *IET Commun.*, vol. 12, no. 7, pp. 816–823, Apr. 2018.
- [8] M. Tlich, A. Zeddani, F. Moulin, and F. Gauthier, "Indoor power-line communications channel characterization up to 100 MHz, Part II: Time-frequency analysis," *IEEE Trans. Power Del.*, vol. 23, no. 3, pp. 1402–1409, Jul. 2008.
- [9] B. Tan and J. Thompson, "Power line communications channel modelling methodology based on statistical features," [Online]. Available: <http://arxiv.org/pdf/1203.3879.pdf>
- [10] L. Lampe and A. J. HanVinck, "Cooperative multihop power line communications," in *Proc. IEEE Int. Symp. Power Line Commun. Appl.*, Beijing, China, Mar. 2012, pp. 1–6.
- [11] P. Karols, K. Doster, G. Griepentrog, and S. Huettinger, "Mass transmit power traction networks as communication channels," *IEEE J. Sel. Areas Commun.*, vol. 24, no. 7, pp. 1339–1350, Jul. 2006.
- [12] W. Muenthetrakoon, K. Khutwiang, and C. Kotchasarn, "SER of multi-hop decode and forward cooperative communications under Rayleigh fading channel," in *Proc. 2nd Int. Conf. Intell. Syst., Model. Simul.*, Jan. 2011, pp. 318–323.
- [13] Y. Ai and M. Cheffena, "Capacity analysis of PLC over Rayleigh fading channels with colored Nakagami- m additive noise," in *Proc. IEEE 84th Veh. Technol. Conf.*, Sep. 2016, pp. 1–5.
- [14] N. Agrawal, P. K. Sharma, and T. A. Tsiftsis, "Multihop DF relaying in NB-PLC system over Rayleigh fading and Bernoulli-Laplacian noise," *IEEE Sys. J.*, vol. 13, no. 1, pp. 357–364, Mar. 2019.
- [15] M. Gotz, M. Rapp, and K. Dostert, "Power line channel characteristics and their effect on communication system design," *IEEE Commun. Mag.*, vol. 42, no. 4, pp. 78–86, Apr. 2004.
- [16] H. Meng, Y. L. Guan, and S. Chen, "Modeling and analysis of noise effects on broadband power-line communications," *IEEE Trans. Power Del.*, vol. 20, no. 2, pp. 630–637, Apr. 2005.
- [17] A. Dubey, R. K. Mallik, and R. Schober, "Performance of a PLC system in impulsive noise with selection combining," in *Proc. IEEE Glob. Commun. Conf.*, Anaheim, CA, USA, Dec. 2012, pp. 3508–3512.
- [18] A. Dubey, R. K. Mallik, and R. Schober, "Performance analysis of a power line communication system employing selection combining in correlated log-normal channels and impulsive noise," *IET Commun.*, vol. 8, no. 7, pp. 1072–1082, May 2014.
- [19] B. Nikfar and A. J. H. Vinck, "Space diversity in MIMO power line channels with independent impulsive noise," in *Proc. 6th Workshop Power Line Commun.*, Rome, Italy, Sep. 2012, pp. 1–3.
- [20] D. Veronesi *et al.*, "Characterization of in-home MIMO power line channels," in *Proc. IEEE Int. Symp. Power Line Commun. Appl.*, Udine, Italy, Apr. 2011, pp. 42–47.
- [21] S. P. Dash, R. K. Mallik, and S. K. Mohammed, "Coherent detection in a receive diversity PLC system under Nakagami- m noise environment," in *Proc. IEEE Int. Symp. Per., Indoor, Mob. Radio Commun.*, Valencia, Spain, Sep. 2016, pp. 1–6.
- [22] S. P. Dash, R. K. Mallik, and S. K. Mohammed, "Performance analysis of a Gauss-optimal receiver for a receive diversity PLC system in Nakagami- m noise environment," in *Proc. Nat. Conf. Commun.*, Hyderabad, India, Feb. 2018, pp. 1–6.
- [23] Y. Ai, T. Ohtsuki, and M. Cheffena, "Performance analysis of PLC over fading channels with colored Nakagami- m background noise," in *Proc. IEEE Veh. Technol. Conf.*, Sydney, NSW, Jun. 2017, pp. 1–6.
- [24] Y. Kim, H. M. Oh, and S. Choi, "BER performance of binary transmitted signal for power line communication under Nakagami-like background noise," in *Proc. Energy: 1st Int. Conf. Smart Grids*, Green Commun. IT Energy-Aware Technol., Venice, Italy, May 2011, pp. 126–129.
- [25] Y. Kim, H. M. Oh, and S. Choi, "Error rate performance of QPSK transmitted signal for power line communication under Nakagami-like background noise," in *Proc. Energy: Second Int. Conf. Smart Grids*, Green Commun. IT Energy-Aware Technol., St. Maarten, The Netherlands, Mar. 2012, pp. 29–33.
- [26] S. P. Dash, R. K. Mallik, and S. K. Mohammed, "Performance analysis of coherent PLC with MPSK signaling in Nakagami- m noise environment," *IEEE Trans. Veh. Technol.*, vol. 69, no. 3, pp. 3057–3067, Mar. 2020.
- [27] B. R. Reddy and S. P. Dash, "Optimal QPSK constellation for a PLC System in Nakagami- m noise environment," *IEEE Commun. Lett.*, vol. 24, no. 6, pp. 1206–1210, Jun. 2020.
- [28] L. I. Rajeshwari, K. P. Vittal, and U. Sripathi, "A low SNR approach to substation communication using powerline for EMI reduction," in *Proc. Asia-Pacific Symp. Electromag. Compat.*, Singapore, May 2012, pp. 453–456.
- [29] G. Prasad, H. A. Latchman, Y. Lee, and W. A. Finamore, "A comparative performance study of LDPC and Turbo codes for realistic PLC channels," in *Proc. IEEE Int. Symp. Power Line Commun. Appl.*, Glasgow, U.K., Apr. 2014, pp. 202–207.



Soumya P. Dash (Member, IEEE) received the B.Tech. degree in electrical engineering from the Indian Institute of Technology, Bhubaneswar, in 2014 and the Ph.D. degree in electrical engineering from the Indian Institute of Technology, Delhi, in 2019. From January 2019 to March 2019, he was an Early-Doctoral Research Fellow with the Department of Electrical Engineering, Indian Institute of Technology, Delhi. Since March 2019, he has been with the faculty of the School of Electrical Sciences, Indian Institute of Technology, Bhubaneswar, where he is currently an Assistant Professor. His research interests include communication theory for hybrid communication systems, power line communications, smart grid communications, next-generation wireless communication systems, and diversity combining. He is a Member of the IEEE Communications and Vehicular Technology Societies.



Ranjan K. Mallik (Fellow, IEEE) received the B.Tech. degree in electrical engineering from the Indian Institute of Technology Kanpur, in 1987, and the M.S. and Ph.D. degrees in electrical engineering from the University of Southern California, Los Angeles, in 1988 and 1992, respectively. From 1992 to 1994, he was a Scientist with the Defence Electronics Research Laboratory, Hyderabad, India, working on missile and EW projects. From November 1994 to January 1996, he was a Faculty Member with the Department of Electronics and Electrical Commu-

nication Engineering, Indian Institute of Technology, Kharagpur. From January 1996 to December 1998, he was with Faculty, Department of Electronics and Communication Engineering, Indian Institute of Technology, Guwahati. Since December 1998, he has been with the faculty of the Department of Electrical Engineering, Indian Institute of Technology, Delhi, where he is currently an Institute Chair Professor. His research interests include diversity combining and channel modeling for wireless communications, space-time systems, cooperative communications, multiple-access systems, power line communications, molecular communications, difference equations, and linear algebra.

He is a Member of Eta Kappa Nu. He is also a Member of the IEEE Communications, Information Theory, and Vehicular Technology Societies, the American Mathematical Society, and the International Linear Algebra Society, the Indian National Academy of Engineering, the Indian National Science Academy, The National Academy of Sciences, Prayagraj, India, the Indian Academy of Sciences, Bengaluru, India, The World Academy of Sciences-for the advancement of science in developing countries, The Institution of Engineering and Technology, U.K., The Institution of Electronics and Telecommunication Engineers, India, and The Institution of Engineers, India, and a Life Member of the Indian Society for Technical Education. He was the recipient of the Hari Om Ashram Prerit Dr. Vikram Sarabhai Research Award in the field of electronics, telematics, informatics, and automation, the Shanti Swarup Bhatnagar Prize in engineering sciences, the Khosla National Award, and the J. C. Bose Fellowship. He has served as an Area Editor and an Editor of the IEEE TRANSACTIONS ON WIRELESS COMMUNICATIONS, and as an Editor of the IEEE TRANSACTIONS ON COMMUNICATIONS.



Badri Ramanjaneya Reddy received the B.Tech. degree in 2017 in electronics and communication engineering from the Rajiv Gandhi University of Knowledge Technologies, RK Valley, India and the M.Tech. degree in 2020 in electronics and communication engineering from the Indian Institute of Technology, Bhubaneswar, where, he is currently working toward the Ph.D. degree in electronics and communication engineering. His research interests include next generation wireless communication, quantum communication, and power line communication.